

# Direct Observation of Steady-state Microtubule Dynamics

David Kristofferson, Tim Mitchison, and Marc Kirschner

Department of Biochemistry and Biophysics, University of California, San Francisco, California 94143

**Abstract.** Different types of unusual dynamic behavior have been reported for steady-state microtubules. While almost all earlier reports relied on kinetic measurements of bulk polymerization, we have directly visualized the steady-state addition of subunits to individual microtubules through the use of tubulin derivatized with biotin. Biotinylated tubulin was used both as an internal "seed" for polymerization and as a marker for assembly onto the ends of microtubules composed of purified tubulin. Biotinylated segments were distinguished from unmodified tubulin by double-label immunofluorescence. Microtubule lengths, number concentrations, and segment lengths have

been monitored with time at steady state under two buffer conditions. The results indicate that the microtubule steady state under these conditions is a balance between a majority of slowly growing microtubules and a minority of rapidly depolymerizing ones as described by the "dynamic instability" model (Mitchison T., and M. Kirschner, 1984, *Nature (Lond.)*, 312:232-242). Microtubules show no evidence of treadmilling; instead most show progressive growth off both ends at steady state. Although solvent conditions markedly influence the growth rates, qualitatively the behavior is unchanged.

**I**N the past few years, biophysical studies of actin and tubulin have focused on the role of nucleotides and their hydrolysis during assembly. The picture of a polymer in simple equilibrium with its subunits as described by Oosawa and Asakura (22) has been replaced by more complicated dynamic models that envisage a steady state with accompanying nucleotide hydrolysis. Wegner (25) first advanced the possibility that such a steady state could involve head-to-tail polymerization. In this model for actin, hydrolysis of proto-mer-bound nucleoside triphosphate, postulated to occur instantaneously after subunit addition, results in simultaneous balanced growth and depolymerization at opposite ends of the same polymer. Margolis and Wilson (18) proposed a similar opposite end assembly-disassembly or "treadmilling" mechanism to account for the continuous uptake and loss of subunits by microtubules (MTs)<sup>1</sup> at steady state. The requirement of nucleotide hydrolysis for subunit uptake was shown experimentally with nonhydrolyzable GTP analogs (5, 17, 24) and the contribution of diffusional subunit exchange at MT ends has been studied extensively (27).

Recently, an alternative interpretation of MT steady-state dynamics was proposed by Mitchison and Kirschner (19). The model is based on observations of individual MT behavior when the free tubulin concentration is equal to or below the steady-state concentration. This new "dynamic instability" model asserts that the steady state consists of a balance between two phases: a majority of MTs which are slowly growing and a minority which are rapidly shrinking. Growing MTs are thought to have tubulin subunits with bound GTP

at the polymer ends. The terminal subunits in shrinking MTs are thought to have bound GDP. MTs can transit between the two phases stochastically by fluctuations in the amount of terminal tubulin-GTP (TbGTP) subunits. The model is based in large measure on the recent ideas about the existence of GTP subunits at the end of the polymer (GTP caps) (3), the ability of terminal subunits with bound GTP to stabilize MTs, and the existence of two kinetic phases of MT growth (2, 4, 8). Monte Carlo simulations of the system using reasonable rate constants generate the dynamic instability behavior (7). When the steady state was analyzed experimentally, it was found to be quite dynamic (19). At the plateau in turbidity, the number concentration and length of MTs changed continuously. These drastic subunit rearrangements might possibly explain the subunit incorporation results previously attributed to treadmilling.

To observe these dynamic changes at steady state, bulk measurements such as turbidity, sedimentation, or viscometry are not very useful since the overall polymer mass is constant. It was necessary to look at the MT length distribution and number concentration directly by microscopy. However, such measurements still lack the detail needed to reveal which end of an MT is growing or shrinking and at what rate. Other possible phenomena that could account for changes in MT number and length, such as end-to-end MT annealing, would be difficult to detect. In this study, we have used biotinylated tubulin (biot-Tb) and double-label immunofluorescence to visualize directly the sites of subunit addition at steady state. Treadmilling and dynamic instability make very different predictions about the sites, rates, and persistence of subunit addition. We have used the pulse-labeling method to evaluate

<sup>1</sup> Abbreviations used in this paper: biot-Tb, biotinylated tubulin; MAP, microtubule-associated protein; MT, microtubule; PC-Tb, phosphocellulose-purified tubulin; TbGTP (GDP), tubulin bound with GTP (GDP).

the possible contributions of both phenomena and to help refine our understanding of MT growth. In the following experiments, unlabeled tubulin is added to biot-Tb seeds or biot-Tb is added to unlabeled MTs in either of two different buffer conditions. Under all conditions, MTs continue to grow from both ends at steady state, balancing the decline in MT number concentration. Such continuous growth and catastrophic depolymerization is predicted by the theory of dynamic instability.

## Materials and Methods

### Materials

*N*-Hydroxysuccinimidyl biotin was obtained from Polysciences, Inc., Warrington, PA; Texas red-conjugated streptavidin from Bethesda Research Laboratories, Gaithersburg, MD; and rabbit anti-biotin antibody from Enzo Biochem, Inc., New York, NY. Mouse monoclonal antibody against  $\beta$ -tubulin was a kind gift of S. Blose (Protein Databases, Inc., Huntington Station, NY). Rhodamine- and fluorescein-conjugated secondary antibodies were obtained from Cappel Laboratories, Cochranville, PA.

### Tubulin Preparation

Phosphocellulose-purified tubulin (PC-Tb) was prepared from bovine brains by a modification of the procedure of Weingarten et al. (26) as described in reference 20. Protein concentrations were determined by the method of Bradford (1) using tubulin standards depleted of exogenous nucleotide and calibrated with an extinction coefficient of 1.15 liters/g per cm at 274 nm in 6 M guanidine hydrochloride (14). This calibration method gave concentrations slightly lower (0.8  $\times$ ) than obtained using bovine serum albumin standards as in Mitchison and Kirschner (20). Tubulin concentrations quoted from that paper have been reduced by 0.8  $\times$  in this report.

### Preparation of Microtubule Seeds

Tubulin (~5 mg/ml) in glycerol buffer (30% [vol/vol] glycerol, 80 mM Pipes, 10 mM MgCl<sub>2</sub>, 1 mM EGTA, pH 6.8 with KOH at room temperature) and 1 mM GTP was assembled at 37°C for 30 min and then sheared by three passes through a 3.8-cm 22-gauge needle with ~5 cm of attached Teflon tubing. To initiate assembly of tubulin in Pipes buffer (80 mM Pipes, 1 mM MgCl<sub>2</sub>, 1 mM EGTA, pH 6.8 with KOH at room temperature), 10  $\mu$ l of seeds in glycerol buffer were added to 1 ml of tubulin pre-equilibrated at 37°C in Pipes buffer with 1 mM GTP, 10 mM acetyl phosphate, and 2 IU acetate kinase. Assembly was monitored at 350 nm in a Hewlett-Packard 8450A UV/VIS Spectrophotometer (Hewlett-Packard Co., Palo Alto, CA).

### Preparation of biot-Tb

30 mg of PC-Tb in 10 ml of glycerol buffer and 1 mM GTP were assembled for 30 min at 37°C. 80  $\mu$ l of a solution of *N*-hydroxysuccinimidyl biotin (100 mg/ml in dimethyl sulfoxide) was added with rapid mixing to the assembled MTs. After an additional 15 min at 37°C, 100 mg of sodium glutamate were dissolved in the solution to quench excess reagent. This procedure gave a biotin/tubulin dimer ratio of ~3:1 as measured using [<sup>14</sup>C]*N*-hydroxysuccinimidyl biotin (6). The labeled MTs were sedimented through 4.5-ml sucrose cushions (50% wt/vol in Pipes buffer containing 10 mg/ml sodium glutamate) in a Beckman 50 Ti rotor at 49,000 rpm, 35°C, for 2 h. Pellets were resuspended in 1 ml (total volume) of cold Pipes buffer and homogenized by hand in a Teflon homogenizer. GTP (1 mM) was added and the protein left on ice for 20 min prior to a second spin at 49,000 rpm, 4°C, for 15 min. The supernatant was adjusted to glycerol buffer and 1 mM GTP, and then assembled at 37°C for 30 min. The assembled tubules were centrifuged through sucrose as before except that glutamate was omitted from the cushion. The pellet was resuspended in a minimal amount of Pipes buffer (~1 ml typically), homogenized, and left on ice for 20 min prior to a final 4°C spin as before. The cold supernatant plus 0.1 mM GTP was aliquoted, frozen in liquid nitrogen, and stored at -80°C until use. A typical yield was 8 mg of biot-Tb (25%).

### Slide Preparation and Immunofluorescence

All pipetting of MTs in this procedure was carried out with cut-off Pipetman tips (hole diameter 1-2 mm) to minimize shear. First, 10  $\mu$ l of MTs were added to 90  $\mu$ l of 1% glutaraldehyde in Pipes buffer at 37°C. The sample was mixed gently by inverting the tube a few times and placed at room temperature for 3

min. The fixed MTs were diluted 2-3  $\times$  10<sup>5</sup> fold (depending on the MT concentration) into 4°C Pipes buffer and duplicate 100- $\mu$ l aliquots were spun onto poly-D-lysine-coated coverslips in the Beckman Airfuge EM rotor (30 psi, 15 min). This quantitatively sedimented all the MTs in the aliquot onto the coverslip (19). After a 4-min postfixation in -20°C methanol, the coverslips were rinsed briefly with antibody buffer (150 mM NaCl, 20 mM Tris-HCl, pH 7.4 containing 0.1% Triton X-100 and 1% bovine serum albumin [Sigma A-7638]). biot-Tb was labeled with either Texas Red-streptavidin (3  $\mu$ g/ml in antibody buffer for 30 min) or rabbit anti-biotin (1:100 in antibody buffer for 30 min). The latter reagent allowed greater signal amplification by secondary and tertiary antibody staining, although the signal from the former reagent was often sufficient. When Texas Red-streptavidin was used, after 30 min the streptavidin was removed and a mouse monoclonal to  $\beta$ -tubulin (1:250 in antibody buffer) was added to the coverslip for 20 min. A rinse with wash buffer (antibody buffer without BSA) was followed by fluorescein-conjugated goat anti-mouse at 1:50 in antibody buffer for 15 min. When rabbit anti-biotin was used, the antibody was detected by consecutive incubations with rhodamine-conjugated goat anti-rabbit and rhodamine-conjugated rabbit anti-goat (both 1:50 in antibody buffer for 20 min), followed by mouse anti-tubulin and then fluorescein-conjugated goat anti-mouse as described above. Finally, the coverslips were rinsed again after the goat anti-mouse and mounted in 90% (vol/vol) glycerol, 20 mM Tris, pH 7.9. MTs were photographed on Kodak Tri-X film using the rhodamine and fluorescein filters on a Zeiss Photomicroscope at DIN 37 and 34 respectively. The film was developed in D19.

### Length Measurements

The fluorescein or rhodamine negatives were projected onto transparencies and labeled MT lengths were traced. The segments detected by the other label were projected onto the corresponding transparencies, and the segment lengths were digitized and stored on a computer for subsequent statistical analysis. Because all MTs in the 100- $\mu$ l aliquots were quantitatively sedimented onto coverslips, determination of the average number of MTs per picture frame could be used to calculate the MT number concentration (19). This value together with the average polymer length yielded the polymer mass concentration.

### Axoneme Experiments

Axoneme experiments were performed as in reference 19. Visualization was by immunofluorescence using mouse anti-tubulin and rhodamine-conjugated goat anti-mouse as described above.

### Electron Microscopy

MTs were fixed and diluted about 10<sup>4</sup> fold as for slide preparation above, then 50- $\mu$ l aliquots were centrifuged (Airfuge EM rotor, 30 psi, 15 min) onto 100 mesh parlodion-coated grids. Grids were rinsed on three drops of water, then stained with 1% uranyl acetate, and examined on a Phillips EM 400 microscope.

## Results

### Characterization of biot-Tb

To measure steady-state MT transitions directly, we have made use of a fluorescent probe developed recently (21). Tubulin derivitized with biotin (see Materials and Methods) could be distinguished from unmodified tubulin by fluorescent-labeled biotin-binding proteins, such as streptavidin or anti-biotin antibodies.

biot-Tb has been characterized in two buffers widely used in MT studies. Experiments were performed with either Pipes buffer (80 mM Pipes, 1 mM MgCl<sub>2</sub>, 1 mM EGTA, pH 6.8 with KOH) or glycerol buffer (30% [vol/vol] glycerol [4.1 M], 80 mM Pipes, 10 mM MgCl<sub>2</sub>, 1 mM EGTA, pH 6.8 with KOH), each containing a GTP regenerating system of 1 mM GTP, 10 mM acetyl phosphate, and 2 IU/ml acetate kinase (16). Pipes buffer was used extensively in the earlier work of Mitchison and Kirschner (19, 20) and has the advantage of suppressing spontaneous MT nucleation. Assembly of unmodified tubulin must be initiated by seeding, and then biot-Tb can be added to the pre-existing MT ends with only negligible amounts of new MTs formed de novo. Glycerol

conforms to the Mitchison and Kirschner procedure (19) except for the introduction of biot-Tb, the method is open to two criticisms. Shearing the MTs during assembly exposes the TbGDP cores. These newly created TbGDP ends are unstable. Rapid MT disassembly ensues until the ends are restabilized with TbGTP and assembly recommences. It could be objected that shearing might somehow enhance the subsequent steady-state dynamics observed earlier by Mitchison and Kirschner (19) and in our first experiment here. A second criticism of the method just described concerns the inhibition of dynamics at MT ends by biot-Tb in Pipes buffer.

To overcome these objections, our second experiment used biot-Tb as the seed for the assembly of a vast excess of unmodified tubulin. This removes any perturbation of the kinetics by biot-Tb interacting with MT ends. Shearing was also omitted. The results in both the first and second experiments were similar (see below) except for a slight inhibition in rates when biot-Tb interacted with MT ends. This also indicates that shearing had no unusual effects on the steady-state dynamics.

In our third experiment we examined the steady-state dynamics in glycerol buffer. Because tubulin assembles spontaneously without seeding under these conditions, biot-Tb was added (50:50 final mixture with unmodified tubulin) to MTs previously assembled to steady state. Any other method would have resulted in biot-Tb incorporation along the entire MT under glycerol buffer conditions. As biot-Tb assembles at rates similar to unmodified tubulin in glycerol buffer (Fig. 1C), normal steady-state dynamics should be observed.

Glycerol "seeds" and MTs formed in both buffers appear normal by negative stain electron microscopy. No evidence for non-MT-tubulin polymers is apparent. Shearing assembling MTs has no apparent effect on the morphology of the ensuing steady-state MTs. As the sample preparation protocol is similar for both electron and fluorescence microscopy (Materials and Methods), electron microscopy samples confirm that the fluorescence images are single MTs in almost all cases. This is also evident by fluorescence when biot-Tb is added to MT ends in the first experiment. Unless labeled segments in side-by-side MTs corresponded closely, fluorescent images of unresolvable MT doublets would contain internal biot-Tb segments. Such occurrences are rare as indicated below.

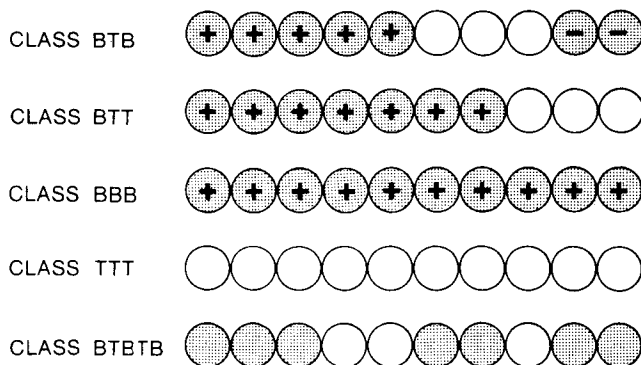


Figure 2. Classification of labeling curves. Incorporation of biot-Tb (shaded circles) into MTs results in five possible labeling configurations. + and - correspond to biot-Tb uptake at the fast- and slow-growing ends, respectively. Open circles represent unmodified tubulin.

**Assembly of biot-Tb onto MT Seeds.** When biot-Tb is added to MT seeds, five general labeling patterns are found which are shown diagrammatically in Fig. 2. The class of MTs with biot-Tb at both ends is termed class BTB, B signifying biot-Tb and T unlabeled tubulin. The presence of biot-Tb at one end is denoted as BTT. Fully labeled polymers are designated BBB and fully unlabeled, TTT. The last class, BTBTB, represents all forms with internal biotin segments. These could arise by annealing or represent artifacts as mentioned above.

Fig. 3A shows PC-Tb in Pipes buffer induced to assemble by the addition of 1/100 vol of MT seeds. The steady-state plateau is reached by shearing the assembling tubules as in reference 19 (Fig. 4). In this instance, after the plateau turbidity level was determined, the microtubules were sheared a second time, and 100  $\mu$ l of 11.1 mg/ml (111  $\mu$ M) biot-Tb in the same buffer at 37°C was added when the turbidity returned to the plateau value. This addition of biot-Tb creates an approximately equimolar mixture of unmodified and biotinylated free tubulin dimers which labels the MT ends. The addition of biot-Tb in an approximately equimolar amount doubles the free total tubulin concentration, but because an

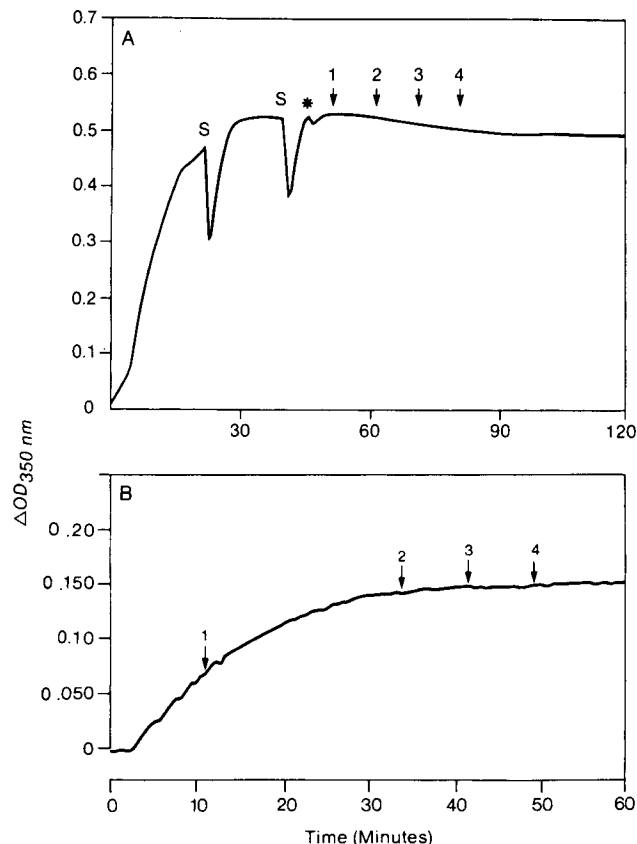


Figure 3. MT assembly curves in Pipes buffer. (A) Assembly of 1 ml of PC-Tb (48  $\mu$ M) at 37°C in Pipes buffer with 1 mM GTP, 10 mM acetyl phosphate, and 2 IU/ml acetate kinase. Assembly is initiated by seeding as in Materials and Methods. MTs were sheared (S) by three passes through a 3.8-cm 22-gauge needle with 5 cm of attached tubing. At the \*, 100  $\mu$ l of 111  $\mu$ M biot-Tb was added. MT aliquots were fixed for immunofluorescence at the four indicated time points spaced at 10-min intervals. (B) Assembly of PC-Tb (1 ml, 25  $\mu$ M) at 37°C. Buffer conditions are the same as in A. Assembly was initiated by adding 10  $\mu$ l of seeds formed from 50  $\mu$ M biot-Tb in glycerol buffer. MTs were not sheared during assembly. MT aliquots were fixed at the indicated time points.

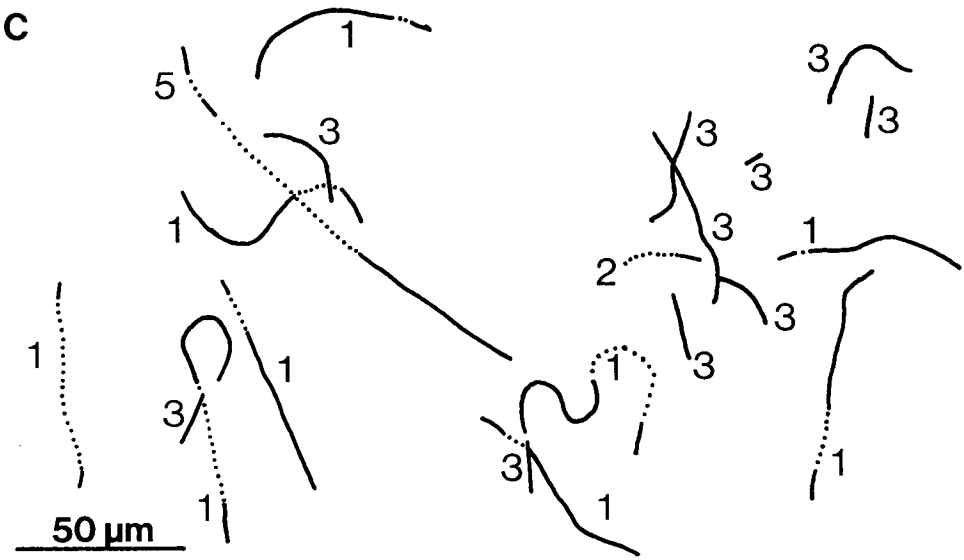
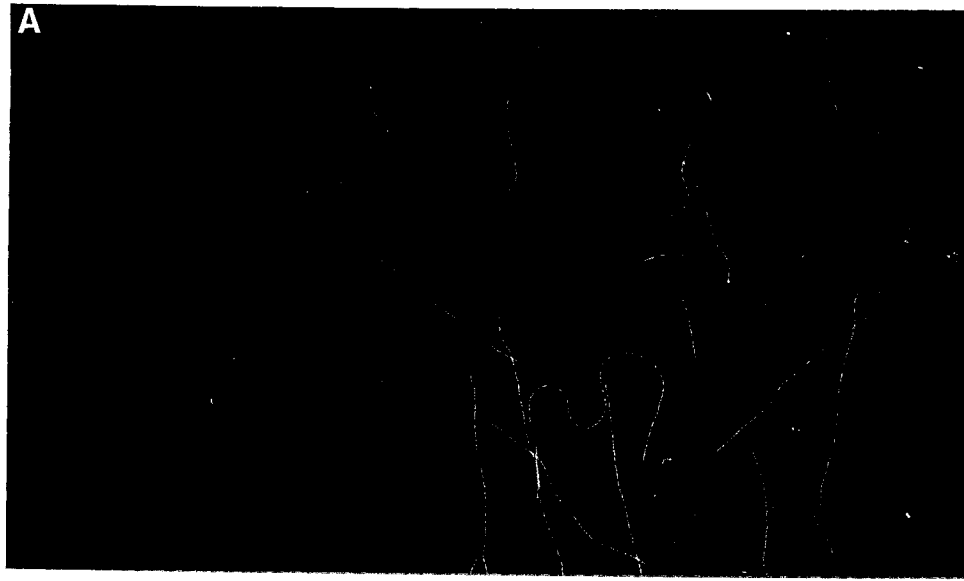


Figure 4. Visualization of MT lengths. (A) Fluorescein signal from anti-tubulin staining reveals the entire MT lengths. (B) Rhodamine signal detects biot-Tb incorporated at the ends of the MTs shown in the previous micrograph. (C) Superposition of A and B. MTs exiting the field were not included. (.....) Tubulin segments. (—) biot-Tb segments. Several microtubules are labeled with their Fig. 2 classification as follows: 1, BTB; 2, BTT; 3, BBB; 4, TTT; 5, BTBTB. No TTT MTs are visible in this field.

equimolar mixture of tubulin and biot-Tb forms ~35–40% less polymer than unmodified tubulin (Fig. 1*B*), very little additional assembly is seen in Fig. 3*A*. In fact, the turbidity plateau shows a slow downward trend. Quantitation of the polymer concentration by microscopy (Table II) confirmed a small loss over 30 min (12%) possibly due to loss of monomer by aggregation as discussed above. Aliquots of MTs were fixed at 10-min intervals during the plateau period. The biotinylated segments and entire MT lengths were visualized as shown in Fig. 4. The overall lengths of labeled and unlabeled segments were measured, and the results are given in Table II. The longer of the two biotinylated segments in BTB microtubules was defined as the plus or fast-growing end and the shorter biotinylated segment was called the minus or slow-growing end. Though it should be kept in mind that these conventions are somewhat imprecise, the over 3:1 ratio of growth rates between plus and minus ends makes it unlikely that ends will be misclassified. The biot-Tb segments of BTT and BBB MTs are also included in the plus end category.

As observed earlier, the average total length of MTs increased rapidly with time and this corresponded to about a 40% drop in number concentration in 30 min, a value which is confirmed by quantitating MT numbers in micrographs. Because the plus and minus end average lengths increased dramatically with time, treadmilling appears not to occur under these conditions.

It is interesting to note in Table II that class BTB and class BBB MTs predominate at all times. At the first time point (zero time) most of the MTs are in class BTB and must either be growing or have recently grown from both ends. The fraction of MTs in this class drops with time (from 71 to 34% in 30 min). The fraction of totally labeled MTs (BBB) increases from 17 to 62%. BTT microtubules decrease in sig-

nificance. Almost all original MT seeds seem to grow since the TTT class is negligible. BTBTB, "annealed", MTs are a small fraction of the total and are dealt with below, separately from the other data in Table II.

THE DISTRIBUTION OF LABELED SEGMENT AND TOTAL LENGTHS. We also examined the length distributions of all segment lengths and total lengths in each MT class. Only the most important results are presented and their significance considered in the Discussion. The overall length distribution of MTs (Fig. 5, *A–D*) becomes more skewed and asymmetric with time. An analysis of similar length distributions in terms of a dynamic instability model with GTP caps has been presented in considerable analytic detail by Chen and Hill (4a). The skewed nature of the distribution is due largely to the BBB class. The average length of BBB MTs is always much less than the overall average (Table II) and the population of this class increases with time.

The interpretation of the data is simplified if instead of looking at the length distribution of all of the MTs one considers only the BTB class. As shown in Fig. 5, *E–H*, this distribution is much more symmetric than the total length distribution though it broadens considerably with time. One can discriminate still further by looking only at the putative plus end of the BTB class (Fig. 6, *A–D*). This distribution has a leading peak which grows at 2.0  $\mu\text{m}/\text{min}$  and a trailing edge which we discuss below. The minus end distribution (not shown) is unimodal and the peak grows at 0.19  $\mu\text{m}/\text{min}$ . The average unmodified tubulin segment length in the middle of the BTB MTs remains constant with time (Table II). The BBB MTs are always shorter than the average (Fig. 6, *E–H*), and the distribution remains skewed in the opposite sense from the plus end distribution of the BTB class. The BBB distribution shows a small but persistent lagging peak and a

Table II. Steady-state Data for MTs in Pipes Buffer: biot-Tb at MT Ends

	Steady-state time points			
	0 min	10 min	20 min	30 min
Avg. MT length ( $\mu\text{m}$ )	32.0 $\pm$ 0.8	38.0 $\pm$ 1.0	47.7 $\pm$ 1.3	50.8 $\pm$ 1.5
Avg. + end length* ( $\mu\text{m}$ )	11.7 $\pm$ 0.2	24.3 $\pm$ 0.5	33.7 $\pm$ 0.8	40.4 $\pm$ 1.1
Avg. – end length ( $\mu\text{m}$ )	2.4 $\pm$ 0.1	4.1 $\pm$ 0.2	5.9 $\pm$ 0.2	8.4 $\pm$ 0.5
MTs in class BTB <sup>‡</sup> (%)	71	54	46	34
MTs in class BTT (%)	11	6	3	4
MTs in class BBB (%)	17	40	51	62
MTs in class TTT (%)	1	0	0	0
Avg. class BBB length ( $\mu\text{m}$ )	11.1 $\pm$ 0.6	20.4 $\pm$ 0.8	27.8 $\pm$ 1.0	35.4 $\pm$ 1.3
Avg. class BTB length ( $\mu\text{m}$ )	36.9 $\pm$ 0.9	51.1 $\pm$ 1.1	70.7 $\pm$ 1.6	80.0 $\pm$ 2.5
Avg. class BTB + end length ( $\mu\text{m}$ )	12.1 $\pm$ 0.2	27.8 $\pm$ 0.5	41.8 $\pm$ 1.1	50.9 $\pm$ 1.9
Avg. class BTB unlabeled length ( $\mu\text{m}$ ) <sup>§</sup>	22.4 $\pm$ 1.0	19.2 $\pm$ 1.4	23.0 $\pm$ 1.9	20.7 $\pm$ 3.2
MT number ( $10^{-10}$ M) <sup>¶</sup>	3.15 $\pm$ 0.06	2.54 $\pm$ 0.06	1.97 $\pm$ 0.15	1.73 $\pm$ 0.05
Polymer conc. ( $\mu\text{M}$ ) <sup>¶</sup>	16.1 $\pm$ 1.0	15.4 $\pm$ 1.1	15.0 $\pm$ 2.4	14.1 $\pm$ 1.2
MTs in class BTBTB(%)**	2.5	2.5	2.0	2.3

\* The + end is defined as the end with the longer of the two biotinylated segments on the MT. The + segments are considerably longer than – end segments so the possibility for confusion is minimal. In the event that an MT is labeled at only one end or completely saturated with biot-Tb, this is also considered a + end length. Errors reported are the SEM ( $s/\sqrt{n}$ ). The overall sample size is 500 MTs at each time point.

<sup>‡</sup> See Fig. 2 definitions of MT classes.

<sup>§</sup> The "unlabeled length" is the length of unmodified tubulin in the MT interior. Values are calculated from the class BTB total, plus, and minus end lengths. Note that only BTB MTs contribute to the minus end average length.

<sup>¶</sup> Determined from the average number of MTs per micrograph (Materials and Methods).

<sup>¶</sup> Determined by microscopy (Materials and Methods). Error limits are calculated from the errors in the average length and in the number of MTs counted per picture frame only. As such they include the major sources of error but do not account for possible errors in the postfixation dilutions.

\*\* Class BTBTB MTs were excluded from the calculations above except in the polymer and number concentration determinations. BTBTB percentages are calculated by including the number of BTBTB MTs noted during the course of measuring the sample of 500 MTs in the other classes, e.g., 13/513 = 0.025 for the 0-min point.

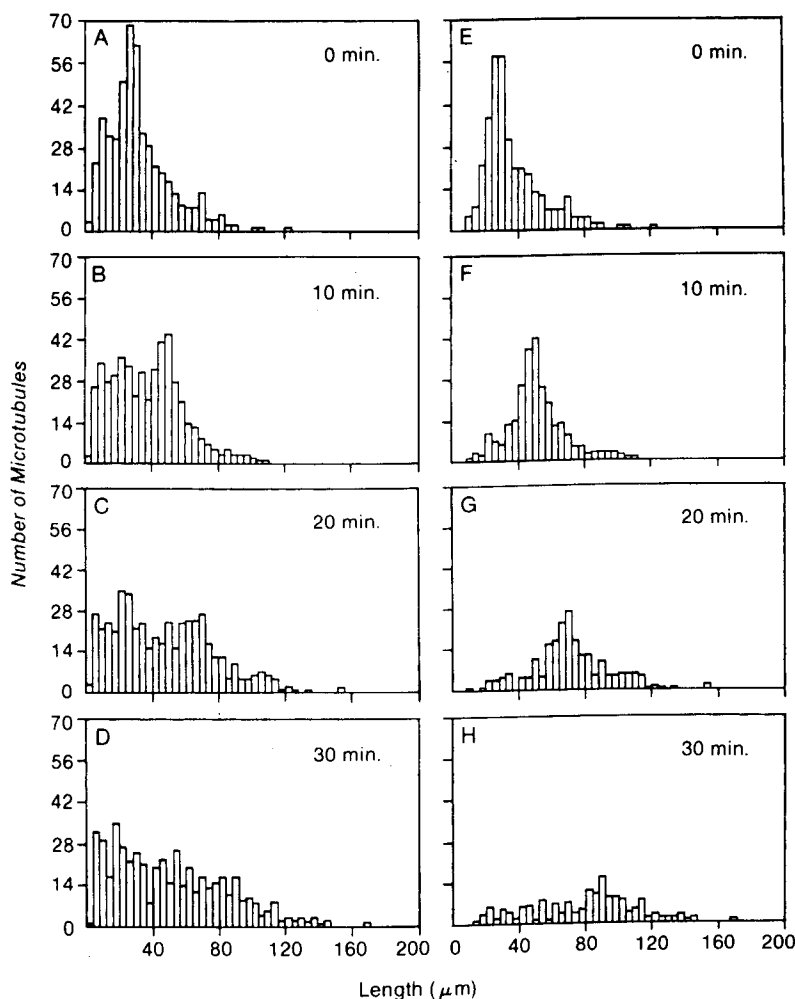


Figure 5. Overall and class BTB MT histograms at steady state. (A–D) Total MT lengths at the 0-, 10-, 20-, and 30-min steady-state time points, respectively. Sample size is 500 in each case and other statistics are in Table II. (E–H) Class BTB MT total length histograms at the corresponding time points. Sample sizes are 357, 269, 229, and 169, respectively. Other data is given in Table II. Note that class BTB MTs are longer than average and show remarkable symmetry in their distributions.

leading edge. Consideration of this detailed behavior will be undertaken in the Discussion.

To determine if BBB MTs resulted from spontaneous nucleation in the presence of biot-Tb at steady state, we measured the rate of MT nucleation in Pipes buffer. An equimolar mixture of biot-Tb and tubulin at 2.0 mg/ml (20  $\mu$ M) was incubated at 37°C for 30 min, the same time period used in Table II. The protein concentration used was actually greater than the expected steady-state concentration of  $\sim$ 1.1 mg/ml (11  $\mu$ M) (19), and thus should overestimate the steady-state nucleation rate. Aliquots were fixed at 10-min intervals, quantitatively centrifuged onto coverslips, and processed for immunofluorescence. The MT number concentration was determined (Materials and Methods) and found to be only 4.2 pM after 30 min. In Table II the concentration of BBB MTs after 30 min is  $0.62 \times 1.73 \times 10^{-10}$  M or  $1.1 \times 10^{-10}$  M. Therefore, <4% of the BBB MTs could have resulted from spontaneous nucleation. Even lower estimates were obtained when pure unmodified tubulin was used in this experiment and in experiments examining the rate of MT appearance in 37°C supernatants after sedimenting out steady-state MTs.

It has been suggested recently that end-to-end annealing might contribute to overall MT length changes at steady state (23). In our system, annealing would also be detectable by the presence of biot-Tb segments in the polymer interior. Such polymers were observed (Fig. 4) but constituted a small fraction of the total. In the course of measuring 500 MTs for each

time point, the number of MTs encountered with internal biot-Tb segments was 13, 13, 10, and 12 at time points 1–4 respectively. Because these represented only 2–3% of the total population, these MTs were not included in the Table II statistical calculations. We conclude that although MT annealing might occur, it is not responsible for the steady-state average length increases.

**MT Steady-state Dynamics in Pipes Buffer using biot-Tb Seeds.** For the second experiment we consider the assembly of a large amount of unmodified tubulin in Pipes buffer initiated with a small volume of biot-Tb MT seeds. The seeded assembly is shown in Fig. 3B. In this experiment, the total concentration of biot-Tb is <3% of the unmodified tubulin concentration and most of the biot-Tb is sequestered in polymer. MTs were assembled to steady state without shearing. In Fig. 3A, shearing the MTs destabilizes them as evidenced by the dips in turbidity in that assembly curve. Presumably, this is due to the exposure of the unstable TbGDP core according to the dynamic instability model. As it could be objected that the dynamics might be influenced by shearing the MTs, we omitted this step here. Note that when shearing is omitted, the turbidity (Fig. 3B) drifts very slowly upwards at steady state due to tubulin aggregation.

As indicated in Fig. 3B, one pre-steady-state and three steady-state MT aliquots were taken for length determinations. The resulting data is shown in Figs. 7 and 8 and Table III. Figs. 7 and 8 show that both plus and minus end segments

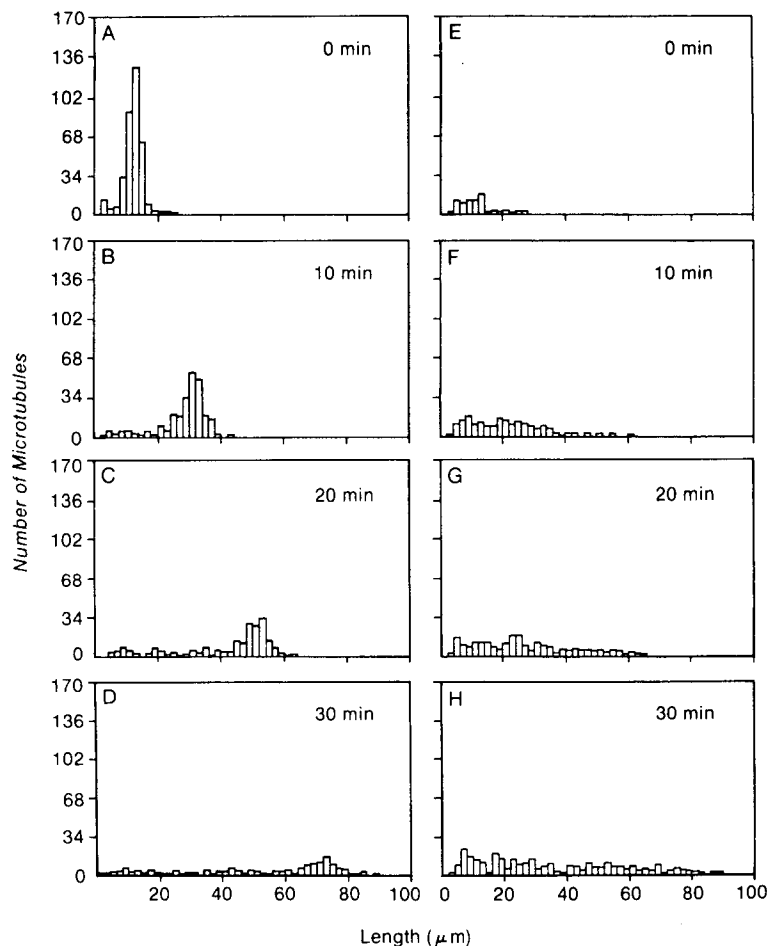


Figure 6. Plus end lengths for classes BTB and BBB. (A-D) Class BTB plus end lengths at the 0-, 10-, 20-, 30-min steady-state time points. Sample sizes are 357, 269, 229, and 169, respectively, and other data is in Table II. Further evidence for class BTB growth is revealed by the shift of the peak in A-D. (E-H) Class BBB lengths (total length = plus end length for class BBB) at the 0-, 10-, 20-, and 30-min time points, respectively. Class BBB MTs are shorter than the overall average at all times. Statistics are compiled in Table II. Sample sizes are 84, 198, 254, and 312, respectively.

elongate at steady state while polymer mass remains constant (Table III), in agreement with the previous experiment. However, when deliberate shearing is omitted from the experimental protocol, the resulting MTs are extremely long. In this experiment, the overall average length increases (Table III) except in the third time point. This raises the possibility that damage occurred to the MT sample during preparation for microscopy. By the first steady-state time point (34 min) a significant number of MTs may have sheared during sample preparation for microscopy as evidenced by the lagging tails in the Fig. 7, A-D, distributions. The shorter minus end distributions (Fig. 7, E-H) do not have trailing edges. Nevertheless, a clear peak is visible in both plus and minus end distribution attesting to continuous steady-state growth at both ends. The plus end growth plot in Fig. 8A is determined by subtracting from each data set the lengths that are significantly shorter than the peak as indicated in the Fig. 7 legend. Both plus and minus end rates are comparable to those in the previous experiment with biot-Tb interacting with MT ends (2.0 and 0.19  $\mu\text{m}/\text{min}$ , respectively), considering the biot-Tb inhibition in the earlier experiment.

A further observation in this experiment is the unexpected plus-to-minus end ratio at steady state. Measurements of tubulin assembly rates off of axonemes (Table I and reference 19) indicate that the plus end grows three-to-four times faster than the minus end. One should note that such experiments are always done under initial rate conditions, i.e., the axoneme concentration is much lower than the tubulin concentration and assembly is monitored during a period in which the

tubulin concentration is essentially constant. We observe a 3.8 plus-to-minus end ratio in the 11-min pre-steady-state time point but this ratio increases when steady state is reached (Table III). This will be considered in the Discussion.

MT annealing in this experiment would be detectable by the appearance of MTs containing two biot-Tb internal segments. Unfortunately, the length of MTs formed by annealing under these conditions would make them likely candidates for mechanical shear during sample preparation, thus complicating a determination of annealing rates. Also, the use of a higher concentration (25  $\mu\text{M}$ ) of unmodified tubulin caused some initial spontaneous nucleation. In the first time point, roughly 25% of the MTs (9 pM) had no biot-Tb cores. Their total lengths were comparable to those of MTs containing biot-Tb cores, suggesting that they were not shear artifacts. Annealing of MTs without biot-Tb markers to MTs containing biot-Tb cores would result in MTs with abnormally long plus or minus ends. MTs of this type and those with two internal biot-Tb cores were tabulated (Table III) but represent a small fraction of the total. While the possibility of shearing complicates an accurate determination of this rate, the continuous smooth growth of the plus and minus end peaks (Fig. 8) makes it unlikely that annealing of the very long MTs in this experiment accounts for the lengthening of both ends at steady state.

*Steady-state Dynamics in Glycerol Buffer.* Finally, we wished to investigate the behavior of MTs in glycerol buffer. biot-Tb more accurately reflects the dynamics of unmodified tubulin under these conditions than in Pipes buffer as seen

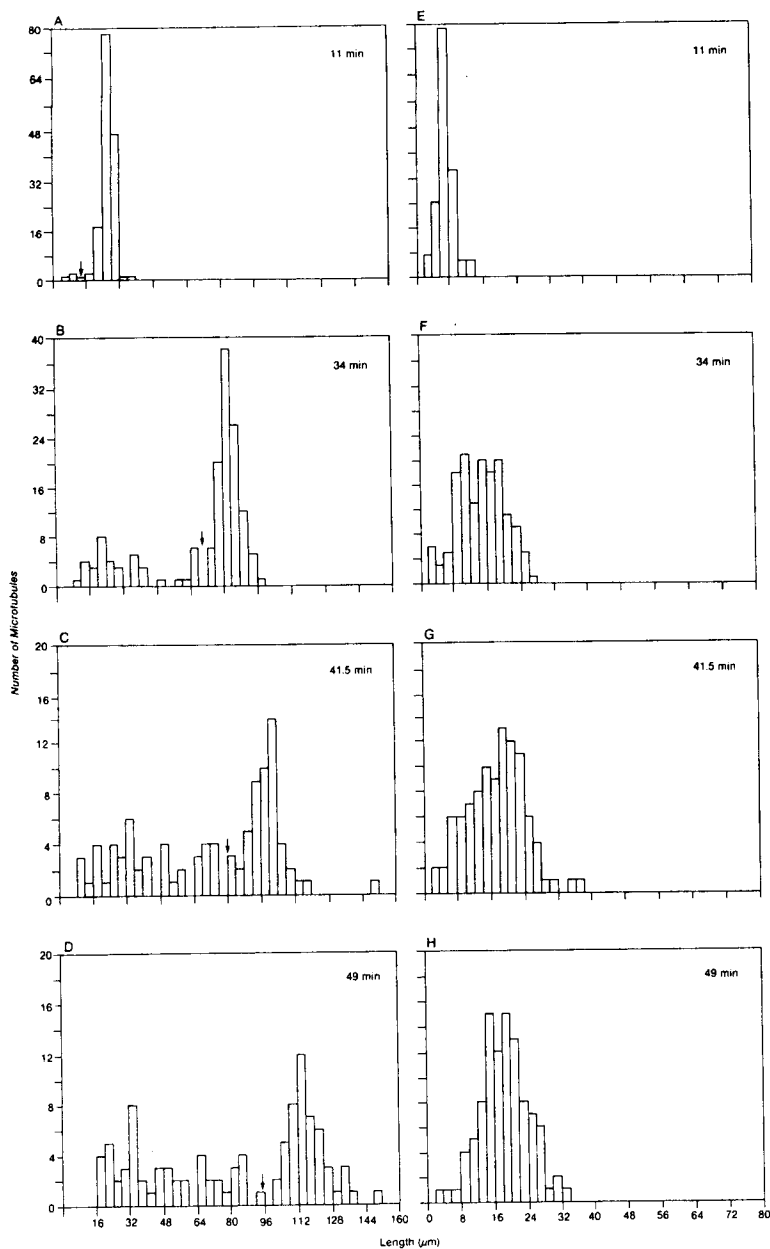


**Figure 7.** Plus and minus end distributions for MTs containing biot-Tb cores (TBT MTs) in Pipes buffer. (A-D) Plus end distributions for the indicated time points. Sample sizes are 150, 150, 100, and 100, respectively. To remove possible shear artifacts when calculating the Fig. 8 plus end growth rates, MTs below certain cut-off lengths were excluded from the average length calculations. These cut-off lengths were 15, 70, 80, and 95  $\mu\text{m}$ , respectively, as indicated by the arrows. (E-H) Minus end length distributions for the indicated time points. Sample sizes as in A-D. No compensation for possible shear was needed with these histograms when calculating the Fig. 8 average lengths.

above. In addition, experiments are not complicated by the aggregation side reaction which occurs in Pipes buffer, so there is no need to shear the MTs to speed assembly. MTs formed under these conditions are fairly short and less likely to break during sample preparation. Most importantly, drastic length redistribution of the Mitchison and Kirschner type (19) had not been studied previously under these conditions, so it was of interest to determine if a possible treadmilling mechanism could occur in glycerol buffer.

An assembly curve in glycerol buffer is shown in Fig. 9. After assembly of PC-Tb (12  $\mu\text{M}$ ) in glycerol buffer to steady state, 100  $\mu\text{l}$  of biot-Tb (46  $\mu\text{M}$ ) was added while still cold to inhibit self-nucleation. This 0.1 vol of cold tubulin causes the transient drop in the turbidity curve; the MTs were not sheared in this experiment. The addition of the biot-Tb produces roughly an equimolar mixture of unmodified and biotinylated free tubulin, since under these conditions the steady-state concentration of free unmodified tubulin is  $\sim 0.5$  mg/ml (5  $\mu\text{M}$ ). After assembly to a new plateau, four samples were

taken at 1-h intervals.

The analysis of segment lengths and total lengths are given in Table IV. Large fluctuations still occur under these conditions, albeit at a reduced rate. The increase in average length over 3 h corresponds to an 18% drop in the number concentration, which was confirmed by quantitative microscopy. Both turbidity (Fig. 9) and microscopy (Table IV) demonstrated that polymer mass remained constant over 3 h. The plus end length increased steadily. The minus end length increased slightly, possibly inhibited by some slight minus end interference of the biot-Tb. The BTB distributions (not shown) have single peaks without trailing edges, indicating that damage to MTs during sample preparation is not significant when the overall lengths are under 20  $\mu\text{m}$ .

The populations of each labeling class are also given in Table IV. Under these conditions of reduced dynamics, the proportion of MTs in the various classes remains virtually unchanged for 3 h (see Discussion). As in the first experiment (Table II) BTB MTs are longer than average and the length

of their unlabeled core remains constant (Table IV). If these MTs were treadmilling, not only would the minus end shorten or disappear (except for the small labeling contribution at that end by diffusional exchange [27]), but the unlabeled core would also shorten by an amount approximately equal to the plus end growth. Because both ends grew and the unlabeled core remained constant, treadmilling under these conditions is effectively excluded.

We also investigated the extent of possible MT annealing under glycerol buffer conditions. The MT number concentration is appreciably higher in glycerol buffer because assembly

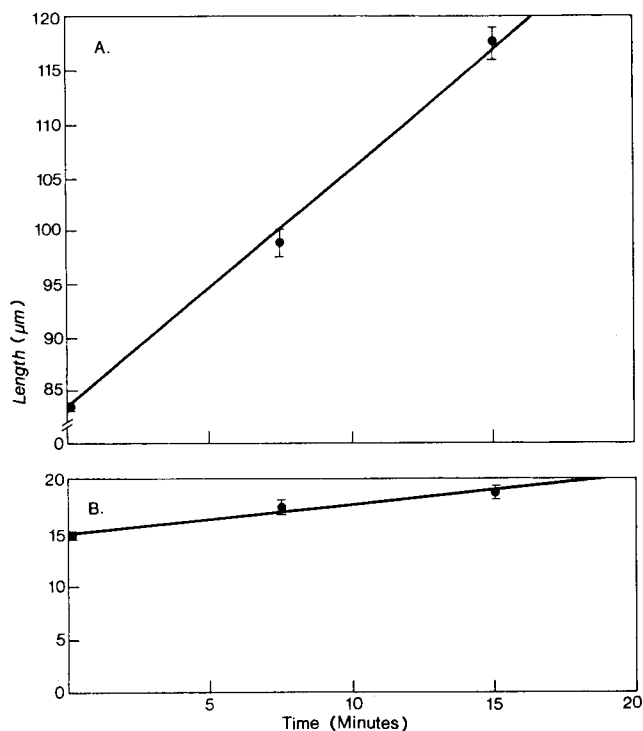


**Figure 8.** Plus and minus end growth rate plots. (A) Plus end averages calculated at steady state using the 34-, 41.5-, and 49-min data in Fig. 7. Averages were corrected for possible shear artifacts as indicated in the legend to Fig. 7, A–D. The 34-min time point corresponds to 0 min at steady state in this plot. The growth rate from a weighted least squares fit is  $2.2 \pm 0.1 \mu\text{m}/\text{min}$ . Each average length in the fit is weighted using its standard error. (B) Minus end averages from the Fig. 7, E–H data. Refer also to the legend of that figure for details. The growth rate from a weighted least squares fit is  $0.26 \pm 0.05 \mu\text{m}/\text{min}$ .

**Table III.** Length Data for Unsheared MTs in Pipes Buffer: biot-Tb Used as Seeds

	Assembly curve time points*			
	11 min	34 min	41.5 min	49 min
Avg. MT length ( $\mu\text{m}$ ) <sup>‡</sup>	$35.8 \pm 0.5$	$71.6 \pm 2.4$	$70.1 \pm 2.7$	$82.8 \pm 3.3$
Number conc. (nM)	$0.036 \pm 0.003$	$0.047 \pm 0.003$	$0.047 \pm 0.005$	$0.037 \pm 0.003$
Polymer conc. ( $\mu\text{M}$ )	$2.0 \pm 0.2$	$5.3 \pm 0.3$	$5.3 \pm 0.5$	$4.9 \pm 0.4$
+ to – end length ratio <sup>§</sup>	3.8	5.7	5.7	6.3
“Annealed” MTs (%) <sup>¶</sup>	2.5	0.5	2.0	1.0

\* Refer to Fig. 3B for time point information.

<sup>‡</sup> Sample size,  $n$ , is 200 for each time point. SEM ( $s/\sqrt{n}$ ) is reported. These samples include MTs with and without biot-Tb cores. 200 MTs were measured for the purpose of calculating number and polymer concentrations. Histograms in Fig. 7 include TBT MTs from this sample plus additional TBT length measurements.

<sup>§</sup> Calculated from the ratio of the plus end peak average length (to remove possible shear artifacts; see Fig. 7, A–D) and the minus end average length.

<sup>¶</sup> Percentage of MTs with two internal biot-Tb segments or abnormally long plus or minus ends encountered during the course of measuring 200 MTs. Lengths of “annealed” MTs were not included in the average length calculations.

is initiated by spontaneous nucleation instead of seeding. This might increase the rate of annealing over Pipes buffer conditions, though the higher viscosity of glycerol buffer may dampen the effect somewhat. In the course of measuring each sample of 500 MTs, 34, 44, 43, and 59 MTs were detected with internal biot-Tb segments at time points 1–4 respectively, but were not included in the averages calculated in Table IV. These levels are about fourfold higher than in the Pipes buffer redistribution experiment, but it was also noted here that several of these MTs had multiple internal biot-Tb segments. Such patterns could not arise from annealing (Fig. 2) unless one postulates the low probability event of three or more MTs joining together. It seems more likely that these patterns are produced by the infrequent cross-linking of MTs side-by-side during fixation and represent an experimental artifact rather than a dynamic phenomenon. The higher MT number concentration in glycerol buffer versus Pipes buffer increases the probability of such an artifact. MT annealing may be taking place at a low rate (10% of the MTs annealed over 3 h), but this cannot explain the lengthening of the other non-annealed MTs. We also strongly emphasize that the biot-Tb is added to MT ends in the overwhelming number of cases under both buffer conditions, and the *in vitro* data lend little support to models which propose appreciable subunit addition directly into MT walls.

## Discussion

We have examined the growth of MTs in Pipes and glycerol buffers and have sought to determine in detail the qualitative behavior of MTs under these conditions. The quantitative differences in polymerization rates between biot-Tb and unmodified tubulin in Pipes buffer as well as the possibility of shearing the long MTs produced under these conditions considerably complicates a comprehensive mathematical analysis. If these problems can be overcome, an attempt at quantitative modeling will be made in the future. The glycerol buffer experiments are not affected by these problems but, unfortunately, the microscopic polymerization rates at the plus and minus ends are not known under these conditions. Consequently, in this report we restrict our scope to mainly a qualitative description of steady-state MT dynamics.

## Pipes Buffer Experiments

Using Pipes buffer, we have demonstrated clearly that the average MT length increases at steady state with growth occurring at both MT ends. A corresponding decline in MT

Table IV. Steady-state Data for MTs in Glycerol Buffer

	Steady-state time points			
	0 h	1 h	2 h	3 h
Avg. MT length ( $\mu\text{m}$ )	14.0 $\pm$ 0.4	14.4 $\pm$ 0.4	15.3 $\pm$ 0.4	17.0 $\pm$ 0.4
Avg. + end length* ( $\mu\text{m}$ )	4.4 $\pm$ 0.1	5.4 $\pm$ 0.2	5.7 $\pm$ 0.2	7.1 $\pm$ 0.2
Avg. - end length ( $\mu\text{m}$ )	1.67 $\pm$ 0.07	1.76 $\pm$ 0.07	1.73 $\pm$ 0.08	2.24 $\pm$ 0.11
MTs in class BTB <sup>‡</sup> (%)	48	55	49	48
MTs in class BTT (%)	27	23	28	31
MTs in class BBB (%)	20	21	19	16
MTs in class TTT (%)	6	2	4	5
Avg. class BTB length ( $\mu\text{m}$ )	17.9 $\pm$ 0.5	18.4 $\pm$ 0.4	19.2 $\pm$ 0.5	21.6 $\pm$ 0.6
Avg. class BTB + end length ( $\mu\text{m}$ )	4.4 $\pm$ 0.2	5.5 $\pm$ 0.2	5.8 $\pm$ 0.2	7.3 $\pm$ 0.3
Avg. class BTB unlabeled length ( $\mu\text{m}$ ) <sup>§</sup>	11.8 $\pm$ 0.5	11.1 $\pm$ 0.5	11.7 $\pm$ 0.6	12.1 $\pm$ 0.6
MT number ( $10^{-10}$ M) <sup>  </sup>	3.41 $\pm$ 0.15	3.51 $\pm$ 0.06	3.00 $\pm$ 0.11	2.93 $\pm$ 0.20
Polymer conc. ( $\mu\text{M}$ ) <sup>  </sup>	7.6 $\pm$ 0.8	8.1 $\pm$ 0.5	7.4 $\pm$ 0.7	8.0 $\pm$ 1.1
MTs in class BTBTB (%)**	6.4	8.1	7.9	10.6

Symbols are defined in legend to Table II.

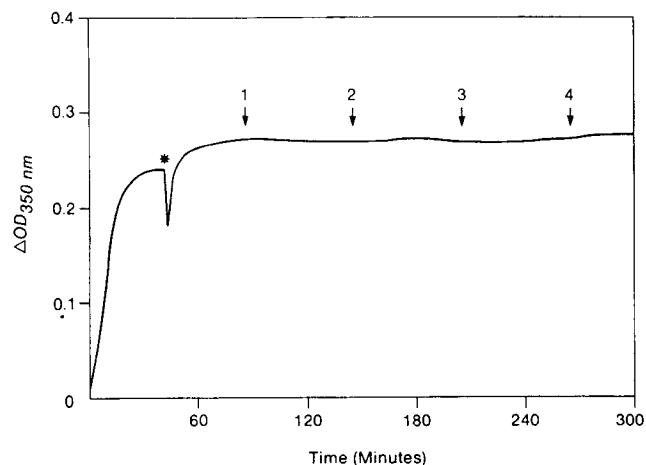


Figure 9. Assembly in glycerol buffer. Assembly of 1 ml of 12  $\mu\text{M}$  PC-Tb at 37°C in glycerol buffer with 1 mM GTP, 10 mM acetate phosphate, and 2 IU of acetate kinase. At the \*, 100  $\mu\text{l}$  of 4°C biot-Tb (46  $\mu\text{M}$ ) is added. biot-Tb is added cold to inhibit self-nucleation. The transient temperature drop causes the dip in turbidity here. MTs are not mechanically sheared. Aliquots for immunofluorescence microscopy length determination are taken at the four indicated 1-h time points.

number concentration maintains constant polymer mass. This result was seen using biot-Tb as an internal marker of MT polarity as well as by the direct incorporation of biot-Tb onto MT seeds, and in the presence and absence of deliberate pre-steady-state MT shear.

The interpretation of the labeling patterns with biot-Tb (Fig. 2) must be done with care. In our first experiment (Table II), most of the MTs in Pipes buffer were found to be in either the BTB class or the BBB class. The BTB population declined with time and the BBB population increased (Table II). The most likely interpretation of the BTB class data is that most of these MTs have not undergone a transition to the shrinking phase. This is indicated by the fact that they retain their labeled segments at each end. BTB plus and minus end distributions both have peaks which grow steadily with time. The leading peak in the plus end distributions (Fig. 6, A-D) grows at a rate of 2.0  $\mu\text{m}/\text{min}$ . This is comparable to the value of 2.2  $\mu\text{m}/\text{min}$  in Fig. 8A with unmodified tubulin and the Mitchison and Kirschner (19) plus end rate of 1.9  $\mu\text{m}/$

min determined at the steady-state concentration in axoneme experiments. The lagging edge of the BTB plus end distribution probably represents MTs damaged during sample preparation but may also include a few which were restabilized after transient depolymerization from their plus ends. Quantitation of such restabilized MTs is difficult because of the possibility of shear artifacts. The minus end distributions show no evidence of tails indicative of possible shear. When biot-Tb interacts with MT ends, the growth rate was 0.19  $\mu\text{m}/\text{min}$ , reflecting some inhibition compared to the 0.26  $\mu\text{m}/\text{min}$  rate with unmodified tubulin in Fig. 8B. Further support for the identification of the BTB class with the growing phase comes from the remarkable symmetry in the class BTB length distributions at each time point (Fig. 5, E-H). Such peaked, symmetric distributions are indicative of MTs growing at a constant rate (11).

BBB MTs are shorter than average. While it is possible that they result from breaking off biot-Tb ends from fixed BTB MTs during sample preparation, some may be restabilized remnants of shrinking phase MTs. This can be shown as follows. If a BTB MT transitioned to the shrinking phase it would first lose a labeled segment at one end and then begin to lose the unmodified tubulin core. In many cases this process continues until the entire MT is lost as evidenced by the large decline in number concentration. However, some MTs might be restabilized and then resume growth. If this happens in the unmodified core, the average length of these interior segments should decrease with time. Instead, the average length of these core segments in BTB MTs is constant despite the sharp decline in overall MT number (Table II). This suggests that any MT which undergoes a transition to the depolymerization phase loses not only its labeled segment at one end (probably the shorter minus end segment) but also the unlabeled core as well. Some of these shrinking MTs might be restabilized after extensive depolymerization into the remaining biot-Tb segment and thus result in BBB tubules labeled completely with biot-Tb. Hill (7) has suggested that MTs might depolymerize from one end until they encounter TbGTP subunits at the opposite end, and then resume polymerization. However, because many BBB MTs may arise as a result of unintentional shearing, it is difficult to determine a rate of restabilization.

It is also possible that BBB MTs may have arisen by new

nucleation in the presence of biot-Tb at steady state. This explanation cannot be valid for an appreciable number of them. We have measured the nucleation rate of tubulin in Pipes buffer at and above steady-state concentrations. The rate is very slow and would give rise to <4% of the observed number of BBB MTs after 30 min. Therefore, most BBB MTs result from either accidental shearing of biot-Tb ends from fixed BTB MTs or from restabilization of shrinking phase MTs as described above.

Whether biot-Tb interacts with MT ends (Fig. 3A) or is used as a seed for the assembly of unmodified tubulin (Fig. 3B) makes no significant difference in the qualitative MT behavior at steady state. We have also used biotin cores (as in Fig. 3B) with pre-steady-state shearing to reach a turbidity plateau rapidly and minimize tubulin aggregation (data not shown). While this protocol produces many MTs without biot-Tb cores, data can be still collected on the subset which retains such cores. Although shearing initially skews the plus-to-minus end ratio in these MTs, the disassembly after shearing, restabilization, and extensive reassembly to steady state re-establishes plus-to-minus end ratios not greatly different from those obtained without shear. In this experiment we have also detected steady-state growth at both ends.

The omission of deliberate shearing when biot-Tb is used for seeding avoids the production of large numbers of MTs without internal markers but results in a slower approach to steady state and very long steady-state MTs. The interruption of the monotonic increase of the overall average length in Table III was noticed only with this protocol. In a second experiment using the same procedure (not shown) the overall average length increases in the first two steady-state time points but declined in the last one. This is a strong indication that the long MTs produced under these experimental conditions are susceptible to accidental shearing during the fixation and preparation steps for microscopy. Despite this problem, when the growth rates of the peaks were analyzed, good agreement was seen between the data from different experiments in Figs. 6 and 7 as described earlier.

The skewing of the growth ratio between the plus and minus ends (Table III) is not understood. The pre-steady-state 11-min time point ratio agrees with initial rate axoneme experiments (Table I), but the later time points do not. Extrapolation from initial rate studies to steady-state values can be justified only if the mechanism of polymerization is invariant. The data indicate that this may not be the case. Growth continues at steady state from both ends but the detailed mechanism of polymerization must change to skew the ratios of growth on the plus and minus ends. A variety of causes could be advanced, but they would be mere speculation at this point.

### *Glycerol Buffer Experiments*

MTs in glycerol buffer show similar behavior to those in Pipes buffer but are clearly less dynamic. Tubulin shows no sign of aggregation or instability under these conditions as evidenced by the over 3-h-long turbidity plateau in Fig. 9. MTs were not sheared in this experiment as indicated in the Fig. 9 legend. We strongly emphasize that the MTs continue to show "dynamic instability" behavior, ruling out both aggregation and shearing to attain steady state rapidly as causes for this phenomenon.

One difference worth noting between the glycerol and Pipes buffer experiments concerns the labeling classes. The origin of BBB MTs is probably different in glycerol buffer. As noted in Fig. 9, biot-Tb was added cold to inhibit self-nucleation, but it is still likely that the BBB MTs in this experiment resulted from spontaneous nucleation in glycerol buffers. The overall MT lengths are far shorter than in Pipes buffer making shear damage unlikely, and no evidence of appreciable shear, e.g., trailing edges as in Fig. 6, A-D, is apparent in the simple unimodal length distributions (not shown). The population of each class (Table IV) is virtually unchanged for 3 h. The fact that the number concentration declines without altering the class populations implies that destabilization of an MT is hard to reverse and usually leads to total disassembly. This would deplete all classes equally. Of course, one cannot rule out other more complex schemes of transitions between classes that might lead to the same result. However, it is most likely that MT restabilization after a growing-to-shrinking transition is a rare event under these conditions. This may also be true in Pipes buffer, but the suspect origin of BBB MTs under those conditions makes a decision difficult. If restabilization is also rare in Pipes buffer then the tails in the Fig. 6, A-D and Fig. 7, A-D distributions are mostly shear artifacts caused during sample preparation.

### *Modulation of Dynamic Instability*

Our data demonstrating extensive length changes at steady state call for a re-evaluation of earlier treadmilling studies using similar conditions (5) because such length redistribution could explain completely the persistent subunit incorporation previously attributed to treadmilling. However, it is important to point out that our results for purified tubulin do not address the question of the effect of microtubule-associated proteins (MAPs) on the system. MAPs or other effectors might give rise to treadmilling even though it is not evident in the pure tubulin polymer. Our results show that the major dynamic changes at steady state occur because of the existence of growing and shrinking phases which interconvert infrequently. If one had sufficiently long MTs (so that they restabilized instead of disappearing while in the shrinking phase) and waited a sufficiently long time, there might be net growth on one end and net loss on the other end, particularly if transitions to the shrinking phase tended to be biased towards one end. Effectors which increase the rate of transitions between growing and shrinking phases could bring these long-term effects into a time scale where one could observe treadmilling.

There is, however, no evidence to date that MAP-MT interactions alter the underlying dynamic instability behavior of pure tubulin to produce treadmilling. Length redistribution in agreement with the dynamic instability model has been observed in at least one tubulin preparation that contains MAPs. Using MT protein purified through initial stages with isotonic buffers (10), Kristofferson and Purich (12) reported a small, but statistically significant steady-state average length increase, in agreement with the "dynamic instability" model. In those experiments, the MT number concentration declined by 7% over 3 h at steady state. Although this rate is even slower than in the glycerol buffer experiment reported here, such a change is still an order of magnitude greater than predicted for a treadmilling model (13). Interestingly, Lee et

al. (15) demonstrated that MTs polymerized from MT protein purified under isotonic conditions are more labile to GDP-induced disassembly than are MTs assembled from other common MT protein preparations. MT "dynamic instability" behavior could be modulated if "uncapped" MT ends composed of TbGDP were not free to disassemble. Whether treadmill results from such modulation remains to be seen. Detailed steady-state length distributions for MAP-containing MTs have only been documented in the literature (12) for "isotonic" tubulin, and in this case the results favor dynamic instability.

The presence of the GTP caps as proposed by Hill and Carlier (8) is at present the most plausible explanation for "dynamic instability." There is still a lingering concern that minor components in our PC-Tb preparation could influence the dynamics. While the contaminant level of PC-Tb is very small compared to the tubulin dimer concentration, some contaminants might be present in a stoichiometric ratio with the MT number concentration in the seeded assembly experiments. Our recent PC-Tb preparations, subsequent to the Mitchison and Kirschner work (19) but used in this paper, have yielded tubulin with somewhat slower assembly rates than reported earlier. We have recently refined our tubulin purification procedures and have reduced the remaining contaminants to exceedingly small levels. This further purification did not greatly alter either tubulin growth rates off of axonemes or steady-state redistribution rates. Although further work on this is in progress, our preliminary results indicate that residual MAPs in PC-Tb do not have a major effect on dynamic instability, and that the phase changes in MTs at steady state are an intrinsic property of tubulin itself.

In summary, for pure tubulin we have shown that the extensive length redistribution at steady state reported in Mitchison and Kirschner (19) is due to growth on both ends of the growing phase MTs, while the overall number concentration declines due to the loss of MTs in the shrinking phase. Growth is persistent and transitions between the growing and shrinking phases are infrequent, often leading to total loss of polymer. MT end-to-end annealing plays a negligible role in the redistribution under both buffer conditions used, although the reaction may occur at a slow rate. MTs do not appear to treadmill in either solvent condition.

We thank Terrell Hill for helpful discussions and Cynthia Hernandez for her fine work in preparing this manuscript.

We thank the National Institutes of Health and the American Cancer Society for their generous support.

Received for publication 5 July 1985, and in revised form 4 November 1985.

## References

- Bradford, M. M. 1976. A rapid and sensitive method for the quantitation

of microgram quantities of protein utilizing the principle of protein-dye binding. *Anal. Biochem.* 72:248-254.

- Carlier, M. F., T. L. Hill, and Y. D. Chen. 1984. Interference of GTP hydrolysis in the mechanism of microtubule assembly: an experimental study. *Proc. Natl. Acad. Sci. USA.* 81:771-775.

- Carlier, M. F., and D. Pantaloni. 1981. Kinetic analysis of guanosine 5'-triphosphate hydrolysis associated with tubulin polymerization. *Biochemistry* 20:1918-1924.

- Chen, Y. D., and T. L. Hill. 1983. Use of Monte Carlo calculations in the study of microtubule subunit kinetics. *Proc. Natl. Acad. Sci. USA.* 80:7520-7523.

- Chen, Y. D., and T. L. Hill. 1985. Theoretical treatment of microtubules disappearing in solution. *Proc. Natl. Acad. Sci. USA.* 82:4127-4131.

- Cote, R. H., and G. G. Borisy. 1981. Head-to-tail polymerization of microtubules *in vitro*. *J. Mol. Biol.* 150:577-602.

- Henderson, R., J. S. Jubb, and S. Whytock. 1978. Specific labeling of the protein and lipid on the extracellular surface of purple membrane. *J. Mol. Biol.* 123:259-274.

- Hill, T. L. 1985. Phase-change kinetics for a microtubule with two free ends. *Proc. Natl. Acad. Sci. USA.* 82:431-435.

- Hill, T. L., and M. F. Carlier. 1983. Steady-state theory of the interference of GTP hydrolysis in the mechanism of microtubule assembly. *Proc. Natl. Acad. Sci. USA.* 80:7234-7238.

- Renumbered in press.

- Karr, T. L., H. D. White, and D. L. Purich. 1979. Characterization of brain microtubule proteins prepared by selective removal of mitochondrial and synaptosomal components. *J. Biol. Chem.* 254:6107-6111.

- Kristofferson, D., T. L. Karr, and D. L. Purich. 1980. Dynamics of linear protein polymer disassembly. *J. Biol. Chem.* 255:8567-8572.

- Kristofferson, D., and D. L. Purich. 1981. Time scale of microtubule length redistribution. *Arch. Biochem. Biophys.* 211:222-226.

- Kristofferson, D., and D. L. Purich. 1981. A quantitative treatment of reversible monomer-polymer exchange reactions with microtubules and other biopolymers. *J. Theor. Biol.* 92:85-96.

- Lee, J. C., R. P. Frigon, and S. N. Timasheff. 1973. The chemical characterization of calf brain microtubule protein subunits. *J. Biol. Chem.* 248:7253-7262.

- Lee, S. H., D. Kristofferson, and D. L. Purich. 1982. Microtubule interactions with GDP provide evidence that assembly-disassembly properties depend on the method of brain microtubule protein isolation. *Biochem. Biophys. Res. Commun.* 105:1605-1610.

- MacNeal, R. K., B. C. Webb, and D. L. Purich. 1977. Neurotubule assembly at substoichiometric nucleotide levels using a GTP regenerating system. *Biochem. Biophys. Res. Commun.* 74:440-447.

- Margolis, R. L. 1981. Role of GTP hydrolysis in microtubule treadmill and assembly. *Proc. Natl. Acad. Sci. USA.* 78:1586-1590.

- Margolis, R. L., and L. Wilson. 1978. Opposite end assembly and disassembly of microtubules at steady state *in vitro*. *Cell.* 13:1-8.

- Mitchison, T., and M. Kirschner. 1984. Dynamic instability of microtubule growth. *Nature (Lond.)* 312:237-242.

- Mitchison, T., and M. Kirschner. 1984. Microtubule assembly nucleated by isolated centrosomes. *Nature (Lond.)* 312:232-237.

- Mitchison, T., and M. Kirschner. 1985. Properties of the kinetochore *in vitro*. I. Microtubule nucleation and tubulin binding. *J. Cell Biol.* 101:755-765.

- Oosawa, F., and A. Asakura. 1975. Thermodynamics of the Polymerization of Protein. Academic Press, Inc. New York. 204 pp.

- Rothwell, S. W., W. A. Grasser, and D. B. Murphy. 1984. Microtubule annealing and subunit flux in labeled microtubules prepared for electron microscopy. *J. Cell Biol.* 99 (4, Pt. 2): 350a. (*Abstr.*)

- Terry, B. J., and D. L. Purich. 1980. Assembly and disassembly properties of microtubules formed in the presence of GTP, 5'-guanylyl imidodiphosphate, and 5'-guanylyl methylendiphosphate. *J. Biol. Chem.* 255:10532-10536.

- Wegner, A. 1976. Head to tail polymerization of actin. *J. Mol. Biol.* 108:139-150.

- Weingarten, M. D., A. H. Lockwood, S. Hwo, and M. W. Kirschner. 1975. A protein factor essential for microtubule assembly. *Proc. Natl. Acad. Sci. USA.* 72:1858-1862.

- Zeeburg, B., R. Reid, and M. Caplow. 1980. Incorporation of radioactive tubulin into microtubules at steady state: experimental and theoretical analyses of diffusional and directional flux. *J. Biol. Chem.* 255:9891-9899.